Biological potential of nanomaterials strongly depends on the suspension media: experimental data on the effects of fullerene C60 on membranes

Article *in* Protoplasma · April 2015
DOI: 10.1007/s00709-015-0803-8 · Source: PubMed

CITATION
1

READS
100

4 authors:

Barbara Drasler
Université de Fribourg
24 PUBLICATIONS **121** CITATIONS
SEE PROFILE

Damjana Drobne
University of Ljubljana
209 PUBLICATIONS **3,806** CITATIONS
SEE PROFILE

Nataša Poklar Ulrih
University of Ljubljana
180 PUBLICATIONS **2,340** CITATIONS
SEE PROFILE

Ajda Ota
University of Ljubljana
26 PUBLICATIONS **153** CITATIONS
SEE PROFILE

Protoplasma
DOI 10.1007/s00709-015-0803-8

ORIGINAL ARTICLE

Biological potential of nanomaterials strongly depends on the suspension media: experimental data on the effects of fullerene C_{60} on membranes

Barbara Drašler[1] · **Damjana Drobne**[1] · **Nataša Poklar Ulrih**[2] · **Ajda Ota**[2]

Received: 16 December 2014 / Accepted: 14 March 2015

Abstract Fullerenes (C_{60}) are some of the most promising carbon nanomaterials to be used for medical applications as drug delivery agents. Computational and experimental studies have proposed their ability to enter cells by penetrating lipid bilayers. The aim of our study was to provide experimental evidence on whether pristine C_{60} in physiological media could penetrate cell membranes. The effect was tested on phospholipid vesicles (liposomes) composed of 1,2-dipalmitoyl-*sn*-glycero-3-phosphocholine, and validated on isolated human red blood cells (RBCs). We incubated the liposomes in an aqueous suspension of C_{60} and dissolved the lipids and C_{60} together in chloroform and subsequently formatted the liposomes. By differential scanning calorimetry measurements, we assessed the effect of C_{60} on the phospholipid thermal profile. The latter was not affected after the incubation of liposomes in the C_{60} suspension; also, a shape transformation of RBCs did not occur. Differently, by dispersing both C_{60} and the phospholipids in chloroform, we confirmed the possible interaction of C_{60} with the bilayer. We provide experimental data suggesting that the suspension medium is an important factor in determining the C_{60}-membrane interaction, which is not always included in computational studies. Since the primary particle size is not the only crucial parameter in C_{60}-membrane interactions, it is important to determine the most relevant characteristics of their effects on membranes.

Keywords Fullerene C_{60} · Liposomes · Human erythrocytes · Experimental medium

Handling Editor: Reimer Stick

✉ Barbara Drašler
barbara.drasler@bf.uni-lj.si

[1] Department of Biology, Biotechnical Faculty, University of Ljubljana, Večna pot 111, SI-1000 Ljubljana, Slovenia

[2] Department of Food Science and Technology, Biotechnical Faculty, University of Ljubljana, Jamnikarjeva 101, SI-1000 Ljubljana, Slovenia

Introduction

With the emerging production of engineered nanomaterials (NMs), there has been an increased concern over the interaction of NMs with biological systems. It has been commonly supposed that the first interactions between cells and NMs occur on the plasma membrane (Banaszak 2009; Verma and Stellacci 2010). Therefore, an understanding of NM-membrane interactions is of the utmost importance, especially due to an increase in the medical applications of NMs, which are used in drug delivery, cellular imaging, biosensor matrices, and other biomedical applications. Carbon NMs are some of the most investigated NMs, prime among them the *buckminsterfullerene* C_{60}. Fullerene C_{60} forms a carbon-based cage structure of about 1 nm, which enables an entrapment of the desired material in drug delivery applications. Furthermore, their unique electrochemical properties (delocalized π-molecular orbital electrons) also make them promising therapeutic agents, such as antioxidants, radical scavengers, or enzyme inhibitors (Bakry et al. 2007; Dellinger et al. 2013; Kato et al. 2010; Kroto et al. 1985; Rossi et al. 2013).

Due to its small size, there has been a rising concern about C_{60} entering the cells by crossing biological membranes. Many theoretical or molecular dynamics (MD) simulation studies report on a successful penetration of C_{60} through phospholipid membranes, an incorporation in the bilayer, or a translocation through the membrane, where, mostly, the

Published online: 02 April 2015

interaction of individual C_{60} molecules is considered (Bouropoulos et al. 2012; DeVane et al. 2010; Monticelli et al. 2009; Qiao et al. 2007; Rossi et al. 2013; Shinoda et al. 2012; Wong-Ekkabut et al. 2008). There are also some MD reports on NM concentration-dependent interactions with membranes, e.g., more highly concentrated C_{60} forming larger clusters (from 10 to a few hundreds nanometers in diameter), which are also prone to permeating through the lipid bilayer (Shinoda et al. 2012; Wong-Ekkabut et al. 2008). Computational studies are good predictors for experimental studies (Bakry et al. 2007; Crane et al. 2008; Lyon et al. 2006; Monticelli et al. 2009; Prato 1997; Rossi et al. 2013; Ruoff et al. 1993). However, under physiological conditions, C_{60} forms large agglomerates, which influence the interactions between C_{60} and biological membranes (Spohn et al. 2009). Recently, Rossi et al. (Rossi et al. 2013) reviewed both experimental and simulation studies and proposed that as the lipid membranes are efficient solubilizing agents for C_{60}, interactions with the lipid bilayer most likely mediate the mechanism of C_{60} toxicity.

Interactions between NMs and membranes are widely studied on both artificial and biological membranes (Drasler et al. 2014; Leroueil et al. 2007; Peetla et al. 2009; Schulz et al. 2012). In NM-membrane interaction studies, NMs can occur (i) encapsulated or entrapped in the liposomes, (ii) in the form of hybrids, composed of inorganic NM and lipids, or (iii) as liposomes, incubated with an aqueous suspension of NMs (Frascione et al. 2012; Wang et al. 2008; Zupanc et al. 2012).

Since it is not possible to visualize C_{60} inside the lipid bilayers directly via microscopy techniques, the indirect effects are inspected to prove the nanoparticle (NP)-membrane interactions. Diverse scattering (e.g., small- or wide-angle X-ray scattering), spectroscopic (e.g., fluorescence polarization, electron paramagnetic resonance), and other techniques are available to study parameters, such as alterations in membrane structure and elasticity or fluidity, respectively. Furthermore, calorimetric techniques, e.g., differential scanning calorimetry, enable an assessment of the alterations of the lipid behavior around phase-transition temperatures, which can indicate a possible incorporation of C_{60} in the bilayer. Synthetic lipid 1, 2-dipalmitoyl-*sn*-glycero-3-phosphocholine (DPPC) is a widely used long-chain phospholipid with a well-characterized gel to liquid-phase transition state (T_m~41 °C; Riske et al. 2009) and thus suitable for studies of the alterations in the phase transition temperature. At the pre-transition temperature (T_p), a flat membrane in the gel phase transforms into a periodically undulated bilayer and corresponds to the alteration of membrane lipids from gel to the liquid crystalline phase at the main-phase transition temperature (T_m) (Riske et al. 2009).

A frequently used experimental model for biological membranes is human erythrocytes (RBCs) (Hagerstrand et al. 2000; Iglic 1997). It has been previously shown that the adsorption of NPs onto the surface of RBCs can change cell morphology (Asharani et al. 2010; Han et al. 2012; Li et al. 2008). As RBCs are the most common type of vertebrate blood cells and C_{60} is considered for medical application as a drug delivery agent, assessing its possible interaction with membranes is of the utmost importance. It has been reported that water-soluble fullerene C_{60} can infiltrate the membranes of human RBCs and change the membranes' fluidity; the membranes can become softer and easier to break, which is also an important reference for the safe application of C_{60} (Huang et al. 1996; Zhang et al. 2013).

The aim of our study was to assess the effects of C_{60} on artificial and biological phospholipid membranes in vitro. Either liposomes or human RBCs were incubated in the aqueous suspensions of C_{60} (distilled water or 10 mM Hepes buffer, pH 7.0), where agglomerates of C_{60} were formed. We studied the interaction of C_{60} with artificial phospholipids by assessing the phase transition profile of DPPC liposomes, and compared it to the potential of C_{60} to affect biological membranes, i.e., to induce a shape transformation of human RBCs. We discuss the importance of experimental conditions in the assessment and interpretation of C_{60} membrane interactions.

Materials and methods

Nanomaterials: suspension preparation and characterization

Fullerenes (C_{60}) in the form of a black crystalline powder (with an estimated nominal purity of >99.5 %) were obtained from Sigma-Aldrich, Steinheim, Germany. A stock solution of C_{60} in chloroform ($CHCl_3$, Merck KGaA, Darmstadt, Germany) was prepared, with a final concentration of 0.16 g/L. This is the solubility limit of C_{60} in $CHCl_3$ at room temperature (Ruoff et al. 1993). Complete solubility was obtained by using 4 mg of powder C_{60} in 25 mL of $CHCl_3$ and applying water bath sonication for 3 h at 30 °C (note, after sonication, the suspension appears clear and purple). A suspension of C_{60} in dH_2O was prepared by dissolving powder C_{60} in deionized water at a concentration of 5 mg C_{60}/mL, followed by probe sonication (Sonics VibraCell, Newtown, ZDA) for 1 h, with 15 s on-off cycles at a 40 % amplitude (cooled on ice). The stock suspensions of C_{60} in phosphate-buffered saline (PBS)-citrate buffer (pH 7.4) were prepared by dissolving powder NM in the buffer, with the final concentration of 2 mg C_{60}/mL.

Transmission electron microscopy (TEM) micrographs were obtained using a JEOL 2100 (Tokyo, Japan), operated at 200 kV. The specimens for TEM were prepared by drying the suspension of NPs in water (pH ~7) at room temperature on a transparent carbon foil supported on a copper grid. Dynamic light scattering (DLS) measurements of the

hydrodynamic sizes of particles in the suspensions (C_{60} in dH_2O, in Hepes buffer—10 mM, pH 7.0, 5 mg/mL, or PBS-citrate buffer—pH 7.4, 5 mg/mL) were performed using a Fritsch Analysette 12 DynaSizer (Idar-Oberstein, Germany). The ζ-potentials of the suspended C_{60} in dH_2O or in PBS-citrate buffer were measured with a Brookhaven Instruments Corp., ZetaPALS (NY, USA).

Experiments with liposomes

Chemicals The lipids 1,2-dipalmitoyl-*sn*-glycero-3-phosphocholine (DPPC) were purchased from Avanti Polar Lipids Inc., USA. Methanol and Hepes buffers were obtained from Sigma-Aldrich (Chemie GmbH, Steinheim, Germany) and chloroform ($CHCl_3$) from Merck KGaA (Darmstadt, Germany). The Hepes buffer solution (10 mM, pH 7.0) was prepared freshly by diluting the powder in deionized water (Milli-Q, Millipore, Billerica, Massachusetts, USA; pH=5.7, ρ=18.5 MΩ/cm) and filtering prior to use (0.22 μm pore size hydrophilic PVDF membrane filters, Millipore, Billerica, Massachusetts, USA). A calibration of the pH value (7.0) of the buffer suspension was carried out using 1 M hydrogen chloride (HCl) and 0.2 M sodium hydroxide (NaOH), both chemicals purchased from Merck KGaA, Darmstadt, Germany.

Preparation of multilamellar vesicles Multilamellar vesicles (MLVs) were prepared by the thin film method, using a rotary evaporator. The DPPC powder lipid was dissolved in chloroform (2 mg DPPC/mL) in a round-bottomed flask, and argon gas was allowed to pass through the lipid-chloroform mixture to avoid the oxidation of lipids. The organic solvent was removed from the flask using the rotary evaporator (BUCHI Rotavapor R-114, Büchi Labortechnik, Flawil, Switzerland) under low pressure (1.7 kPa), until a thin lipid film was formed at the bottom of the flask. The dried lipid film was then hydrated with 1 mL of Hepes buffer (10 mM, pH 7.0). A small amount of silanized glass beads was added to the flask, and the sample was subjected to alternate cycles of vigorous vortexing and heating in a water bath (45 to 50 °C) for 15 min to form MLVs.

For a comparison of the experimental conditions, two exposure approaches were applied. The liposomes were either incubated in an aqueous suspension of C_{60} (i.e., indirect exposure) or first dissolved in $CHCl_3$, followed by the formation of MLVs (i.e., direct exposure).

In the incubation approach, the suspension of MLVs (0.5 mL) formed in Hepes buffer (10 mM, pH 7.0) was added to the suspension of C_{60} in dH_2O (0.5 mL) in a molar ratio of C_{60}:DPPC=1:1 (*n*/*n*). The control samples (the addition of 0.5 mL of dH_2O) were prepared in order to exclude the possible effect of the addition of aqueous suspension to MLVs formed in Hepes buffer (as C_{60} were suspended in dH_2O). For the comparison of C_{60} characteristics in Hepes buffer, the hydrodynamic size of C_{60} (10 mM Hepes buffer, pH 7.0, 0.5 mg/mL) was assessed. The final concentration of DPPC for the differential scanning calorimetry (DSC) measurement in all tested samples was 0.5 mg/mL.

In the direct exposure, where the criteria for a more direct contact between lipids and C_{60} were met, both phospholipids and C_{60}, dissolved in $CHCl_3$, were mixed in a 1:1 M ratio (C_{60}:DPPC=1:1; *n*/*n*; 2 mg/mL DPPC), and the mixture was applied in a round-bottomed flask for the thin film preparation. Then MLVs were formed following the same procedure as in the formation of control MLVs in Hepes buffer (10 mM, pH 7.0).

Differential scanning calorimetry measurements In order to diminish the effect of possibly present air bubbles during the DSC measurements, the samples were first exposed to a low-pressure atmosphere; the vacuum chamber was established using a vacuum pump (Thermolyne Nuova Stirrer, Thermo Scientific, USA). The phase transition temperature of the DPPC MLVs in the absence (control samples) or in the presence of C_{60} was measured using a Nano DS series III calorimeter (Calorimetry Sciences, Provo, UT, USA). The reference cell was filled with Hepes buffer (10 mM, pH 7.0). The samples loaded into the calorimetric cell were heated and cooled repeatedly in the temperature range of 10 to 70 °C, with the heating rate of 1 °C min^{-1}. The phase transition temperatures were expressed on the basis of a measured energy input, required to maintain the same temperature of the reference and sample chamber. The first DSC scan was used to determine the temperature of the gel-to-liquid crystalline phase transition temperature (T_m) of the lipids and the calorimetric enthalpy (ΔH_{cal}), as explained previously (Poklar et al. 1999). The subsequent scans were used to determine the reversibility of the lipid-phase transitions. The OriginPro 9 software (OriginLab Corporation, MA, USA) was used to evaluate the enthalpies and transition temperatures of the lipids from the DSC thermograms. The thermograms were presented in the temperature range from 20 to 60 °C.

Experiments with red blood cells

The alterations in morphology after the exposure to NM were assessed on the basis of our previously published study (Drasler et al. 2014), following the same protocol but with some minor changes. The alterations of the shapes of a red blood cell were assessed by the classification model consisting of the shape types of just two RBCs, i.e., discocytes and non-discoid-shaped erythrocytes (Drasler et al. 2014; Rudenko 2010).

Chemicals NaCl, $NaH_2PO_4 \cdot 2H_2O$, $Na_2HPO_4 \cdot 2H_2O$, and Triton X 100 surfactant (OmniPur) were from Merck KGaA

(Darmstadt, Germany) and KCl and KH_2PO_4 from Kemika (Zagreb, Croatia). The phosphate-buffered saline (PBS-citrate buffer; 137 mM NaCl, 2.7 mM KCl, 7.8 mM $Na_2HPO_4 \cdot 2H_2O$, 1.5 mM KH_2PO_4, pH 7.4) was prepared with the ultrapure distilled H_2O and filtered before use through 0.22 μm pore filters. A modified Karnovsky fixative was prepared from 2.5 % glutaraldehyde, 0.4 % paraformaldehyde, and 1 M Na-phosphate buffer ($NaH_2PO_4 \cdot 2H_2O$ and $Na_2HPO_4 \cdot 2H_2O$). Glutaraldehyde, osmium tetroxide (OsO_4), and hexamethyldisilazane (HMDS) were purchased from SPI Supplies (West Chester, PA, USA). The nanopowder of carbon black (CB; positive control; the primary particle average size of 13 nm and nominal purity >99 %) was provided by PlasmaChem GmbH (Berlin, Germany).

Isolation of human red blood cells Human blood was collected by a medial cubital vein puncture using a 21-gage needle (length 70 mm, inner radius 0.4 mm) (Microlance, Becton Dickinson, NJ, USA) and stored in four 2.7 mL vacutubes containing 0.27 mL trisodium citrate (0.109 mol/L) as an anticoagulant. PBS-citrate buffer was used as the experimental medium in all experiments with RBCs in order to minimize a possible coagulation and a spontaneous deformation of RBCs throughout the experimental procedures. Blood was centrifuged for 20 min in a CENTRIC 400R centrifuge (Domel d.o.o., Železniki, Slovenia) at 150 g and 37 °C to separate the RBCs from the platelet-rich plasma. The RBCs were repeatedly washed three times with PBS-citrate buffer, centrifuged at 1550*g* and 37 °C for 10 min. After the final centrifugation, the excess supernatant was removed and the cells were kept at a room temperature for a maximum of 1 h.

Exposure of RBCs to C_{60} The washed RBCs were diluted with PBS-citrate buffer in a volume-to-volume ratio of 1:1 with the final concentration of ~2×10^9 cells/mL. The samples (0.15 mL) were incubated for 1 h at room temperature in suspensions of C_{60} in PBS-citrate buffer (0.05 mL, the final concentration of C_{60} was 0.5 mg/mL). The positive control samples were incubated with the same volume (0.05 mL) of CB suspension in PBS-citrate buffer (pH 7.4, 0.05 mg/mL) and the negative control samples with PBS-citrate buffer (0.05 mL). Due to the experimental procedure (isolation and fixation) a portion of RBCs already exhibited a slightly altered morphology (Fig. 1a, b), though the majority of cells (more than 80 %) were discocytes (not affected). On the basis of the preliminary results (results not yet published), we used RBCs exposed to CB (nanopowder, size of primary particles ~13 nm) as a positive control to affect the shape transformation of RBCs (more than 20 % of the cells were affected). After the incubation, RBCs were fixed at room temperature for 2 h using a modified Karnovsky fixative. The postfixation of samples was undertaken with 1 % OsO_4. The samples were dehydrated and dried with HMDS; syringes were used to apply samples onto the membrane filters (Isopore Membrane Filters, polycarbonate, filter type 2.00 μm TSTP; Merck KGaA, Darmstadt, Germany). Filters with fixed, dried RBCs were attached to the aluminum holders with silver paint, sputtered with a 30-nm gold-palladium (Precision Etching Coating System Gatan 682, CA, USA), and examined with a field emission scanning electron microscope (SEM; JEOL JSM-6500 F, Tokyo, Japan). The Mann-Whitney test was used to assess the statistical significance of the non-discocyte portion of RBCs between the negative control samples and those exposed to C_{60} or the positive control carbon NM (CB) with similar chemical composition to C_{60}.

Results

Characteristics of C_{60}

The TEM images revealed that the size of the agglomerates of pristine C_{60}, suspended in dH_2O, was from approximately 20 nm to several hundred nanometers in diameter. The DLS measurements of C_{60} suspension in dH_2O (pH 7.1, 0.01 mg/mL) showed a substantial agglomeration with the largest number of particles in the water suspension measuring approximately 80 nm in diameter, with some agglomerates from 100 to 600 nm in diameter also present. C_{60} suspended in PBS-citrate buffer (pH 7.4, 0.5 mg/mL) and in 10 mM Hepes buffer (pH 7.0, 0.5 mg/mL) formed agglomerates larger than 1 μm, which sedimented quickly from the suspension. The DLS measurements of CB suspensions in PBS-citrate buffer (5 mg/mL) showed a relatively broad distribution of hydrodynamic size. The electromobility measurements showed relatively high negative ζ-potential values for C_{60} suspensions, in dH_2O (pH 7.0, 0.1 mg/mL) −26 mV and in PBS-citrate buffer (pH 7.4, 0.1 mg/mL) −28 mV.

Effects of C_{60} on the lipid-phase transition profile

The comparison of the DSC thermograms of control DPPC and the C_{60}-exposed DPPC MLVs is shown in Fig. 2. The DPPC MLVs were either formed in the presence of C_{60}, dissolved in $CHCl_3$ (Fig. 2, dotted line), or incubated in an aqueous suspension of C_{60} (Fig. 2, dashed line). All heating profiles presented with respect to the control sample (pure DPPC MLVs formed in Hepes buffer and diluted with dH_2O) are in good agreement with the reported characteristic values (T_p 35.7±0.2 °C, T_m 41.5±0.5 °C) (Lichtenberg et al. 1984; Boggs 1987; Riske et al. 2009). The thermodynamic profile (T_m and T_p) of the control and the DPPC MLVs exposed to C_{60} is reported in Table 1.

The incubation of the DPPC MLVs in the suspension of C_{60} in dH_2O (C_{60}:DPPC=1:1, *n*/*n*; Fig. 2) did not induce any alterations in the position of the pre-transition or main transition temperature peak with respect to the control (Table 1).

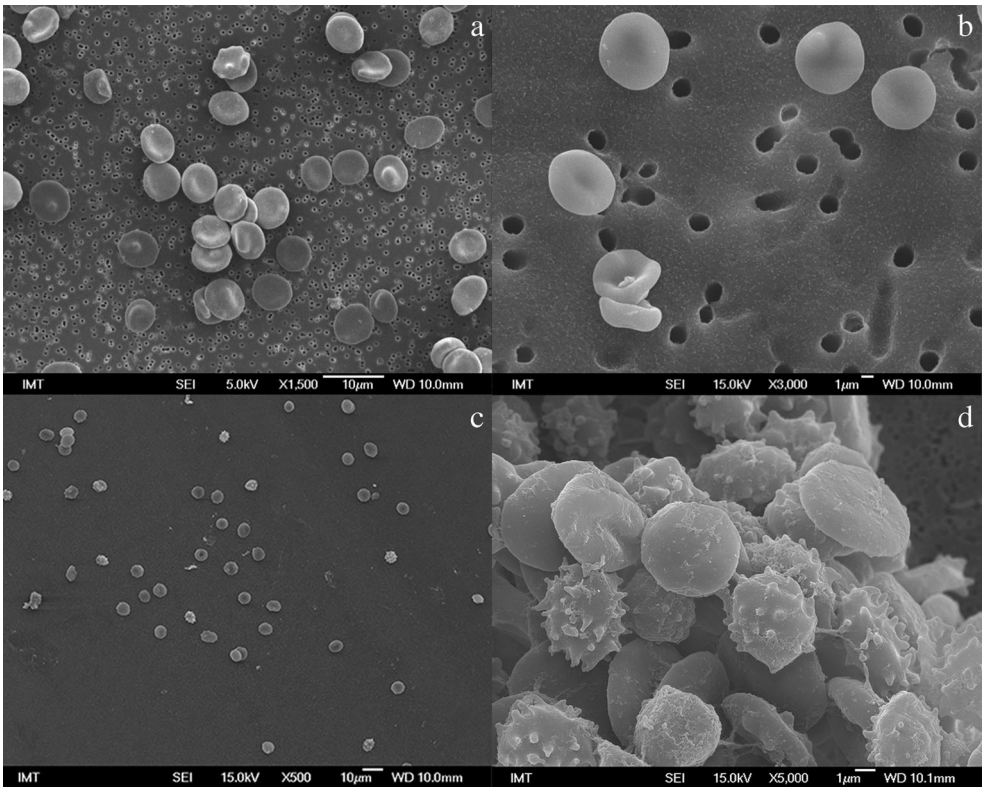

Fig. 1 Scanning electron microscopy image of a randomly chosen region on the scanning electron microscopy holder, on the negative control sample (i.e., human RBCs after 1 h of incubation in PBS-citrate buffer, pH 7.4), at magnification **a** 1500× and **b** 3000×. The majority of red blood cells in the control group (more than 80 % of total) were non-discocytes (not affected). **c** Positive control sample, i.e., RBCs after 1 h incubation in suspension of CB at concentration 0.05 mg/mL, at magnification of 500×, and **d** an example of echinocytes (RBCs with many small, evenly spaced thorny projections) at magnification 5000×. *IMT* Institute of Metals and Technology, Ljubljana, Slovenia, *SEI* secondary electron imaging, *WD* working distance

After the exposure to C_{60} in $CHCl_3$, the main transition peak was broadened, decreased, and shifted towards a lower temperature (from 41.6 to 40.4 °C), while the pre-transition peak was almost eliminated and shifted towards the lower one (36.2 to 34.0 °C).

Effect of C_{60} on morphological changes of RBCs

The exposure of RBCs to C_{60}, suspended in PBS-citrate buffer (pH 7.4, final concentration 0.5 mg/mL), did not induce shape alterations of RBCs, compared to the negative control samples (in PBS-citrate buffer). For comparison, a portion of non-discoid RBCs was significantly higher (Mann-Whitney test, α=0.05; ***p<0.001) in the positive control samples, i.e., exposed to CB (in PBS-citrate buffer, pH 7.4; final concentration 0.5 mg/mL), as shown in Figs. 3 and 4.

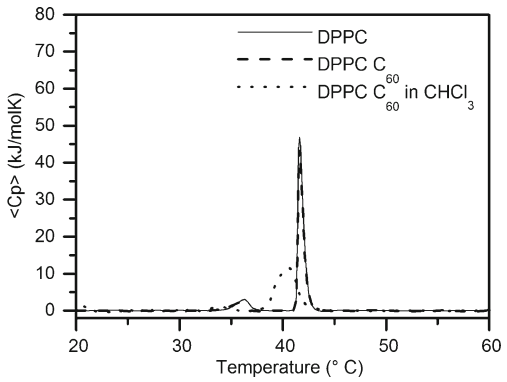

Fig. 2 DSC thermograms for pure DPPC (control MLVs, diluted with dH_2O; full line), DPPC MLVs incubated with the suspension of C_{60} in dH_2O (dashed line), and DPPC MLVs formed in the presence of C_{60} dissolved in $CHCl_3$ (dotted line)

Discussion

Recently, there have been numerous literature reports on the potential of fullerene C_{60} to incorporate in the phospholipid bilayer or enter the cells via translocation through the cell membrane. In this study, we provide experimental evidence showing that the penetration of C_{60} through phospholipid bilayer significantly depends on the medium in which the NPs are suspended. The effect of C_{60} in physiological conditions might not be as prominent as expected (based on the computational studies or from the experiments in biologically non-relevant media). We observed the absence of interaction between C_{60} and artificial or biological membranes after the incubation of liposomes or RBCs in the aqueous suspension of C_{60}. In contrast, the phase transition pattern of DPPC lipids was significantly altered when phospholipids were exposed to C_{60}, both dissolved in the same organic solvent (chloroform).

The interaction between C_{60} and artificial membranes was tested on phospholipid vesicles (liposomes), composed of 1,2-dipalmitoyl-*sn*-glycero-3-phosphocholine, and validated on isolated human red blood cells. We either incubated the liposomes in the aqueous suspension of C_{60}, or first dissolved

Table 1 The thermodynamic profile (T_p and T_m) of the control and the DPPC MLVs exposed to C_{60}

MLV sample	T_p (°C)[a]	T_m (°C)[b]
DPPC control in dH_2O	36.2±0.2	41.6±0.1
DPPC C_{60} in dH_2O	35.3±0.2	41.6±0.1
DPPC C_{60} in $CHCl_3$	34.0±0.2	40.4±0.1

[a] T_p is the pre-transition temperature in which a flat membrane in the gel phase transforms into a periodically undulated bilayer (Riske et al. 2009).

[b] T_m is the main-phase transition temperature required to change the membrane lipids from a gel to a liquid crystalline phase (Riske et al. 2009).

MLV multilamellar vesicles, *DPPC* 1,2-dipalmitoyl-*sn*-glycero-3-phosphocholine, *dH_2O* deionized water, *C_{60}* fullerene C_{60}, *$CHCl_3$* chloroform, T_p pre-transition temperature, T_m main-phase transition temperature

both lipids and C_{60} in chloroform, and subsequently formatted the liposomes. For the purposes of the assessment of the effect of C_{60} on liposomes, the thermal profile (lipid behavior near the phase transition *T*) of phospholipids was assessed using DSC. Alterations in the phase transition temperatures after exposure to C_{60} would signify that the presence of C_{60} affected the phospholipid bilayer, either by intercalation in the hydrophobic region of the membrane (phospholipid tails) or by its adsorption on the hydrophilic part of the bilayer. The phase transition temperature denotes the temperature (T_m) at which an alteration in the phase of membrane lipids occurs, from the ordered gel phase to the disordered liquid crystalline phase. In the gel phase, the hydrocarbon chains are completely extended

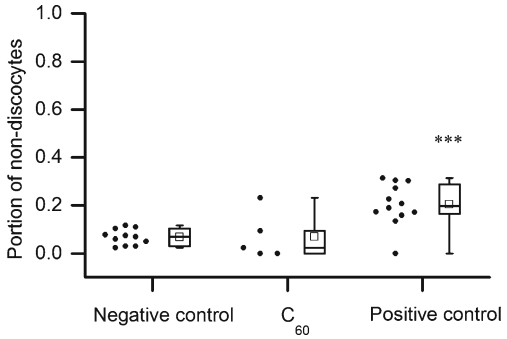

Fig. 3 The percentage of non-discocyte RBCs after the incubation (1 h, 37 °C) in PBS-citrate buffer (negative control), in the suspension of C_{60} in PBS-citrate buffer (0.5 mg/mL), or in the suspension of CB in PBS-citrate buffer (0.5 mg/mL, positive control). *Each dot* presents an analyzed location on the scanning electron microscopy holder. The *y*-axis presents the portion of non-discocyte-shaped RBCs, analyzed on five SEM holders per treatment; on each holder, three locations were analyzed at the magnification of 500. In the negative control group, 1797 RBCs were compared, 276 in the C_{60} group, and 549 in the positive control samples. The *small square in the center of the box plot* represents the mean value, the *central line* is the median *lines* of the box represent the 25th and 75th percentiles. The whiskers are set at two standard deviations from the mean value. The statistical difference in the portion of non-discocytes in the positive control RBCs compared to the negative control samples is marked with *three asterisks* (***$p<0.001$, Mann-Whitney test, $\alpha=0.05$)

and tightly packed, whereas they are loosely packed and more fluid in the liquid crystalline phase (Leonenko et al. 2004). To disrupt the packing order of the lipid chains by different molecules, less energy is required, leading to a decrease in T_m (Gmajner et al. 2011). We used two experimental approaches: (i) i.e., indirect exposure, where the phospholipid liposomes (formed in Hepes buffer beforehand) were incubated in the suspension of C_{60} (in dH_2O), and (ii) i.e., direct exposure, where liposomes were formed from lipids and C_{60}, both dissolved in chloroform. We have observed no alterations in the thermal stability of DPPC when the DPPC MLVs (Hepes buffer, pH 7.0) were incubated with the aqueous suspensions of C_{60} (in dH_2O; $n(C_{60}):n(DPPC)=1:1$). Contrary to the observed absence of interaction of larger fullerene clusters with phospholipid membranes, the phenomenon of biological membranes promoting adsorption and subsequent aggregation of suspended fullerenes has been proven; the formation of microsized fullerene clusters was observed not only inside the cells but also inside cell membranes (Salonen et al. 2008). MD simulation results proposed the aggregation of fullerenes that was mediated by van der Waals interactions between the exposed hydrophobic moieties of the C_{70}-gallic acid assemblies (Salonen et al. 2008). The absence of interactions of larger pristine C_{60} clusters with pure phospholipid membranes could be explained by the different surface characteristics of fullerenes used in these two studies, though additional MD studies considering detailed characteristics of the C_{60} clusters formed in the experimental buffer would be required.

In contrast, with the experimental approach, where the MLVs were formed in the simultaneous presence of both DPPC lipids and C_{60}, dissolved in the same solvent ($CHCl_3$), we set up a non-physiological environment. The expression non-physiological environment signifies that the milieu does not completely meet the criteria for physiological conditions, for example, in terms of pH (6–8), glucose concentration (1–20 mM). Namely, the lipid membranes were exposed to fullerenes after complete dissolvability in the non-polar organic solvent ($CHCl_3$), a condition which does not occur in the human body under normal circumstances. Due to the proven high solubility of C_{60} in the organic solvent ($CHCl_3$; (Ruoff et al. 1993)), we assumed C_{60} molecules were (substantially) evenly dispersed among the phospholipids; therefore, the direct contact of C_{60} with DPPC was enabled prior to the formation of MLVs. We observed that the DPPC peak shapes and positions were affected, suggesting that the incorporation of C_{60} into the bilayer affects the energy of packing of the DPPC lipid membranes. Namely, both the pre- and the main-phase transition temperatures peaks shifted towards lower temperatures; the pre-transition peak was almost eliminated, while the main transition peak was lowered and broadened. Our results regarding C_{60} dissolved in $CHCl_3$ are in line with those of the MD simulation

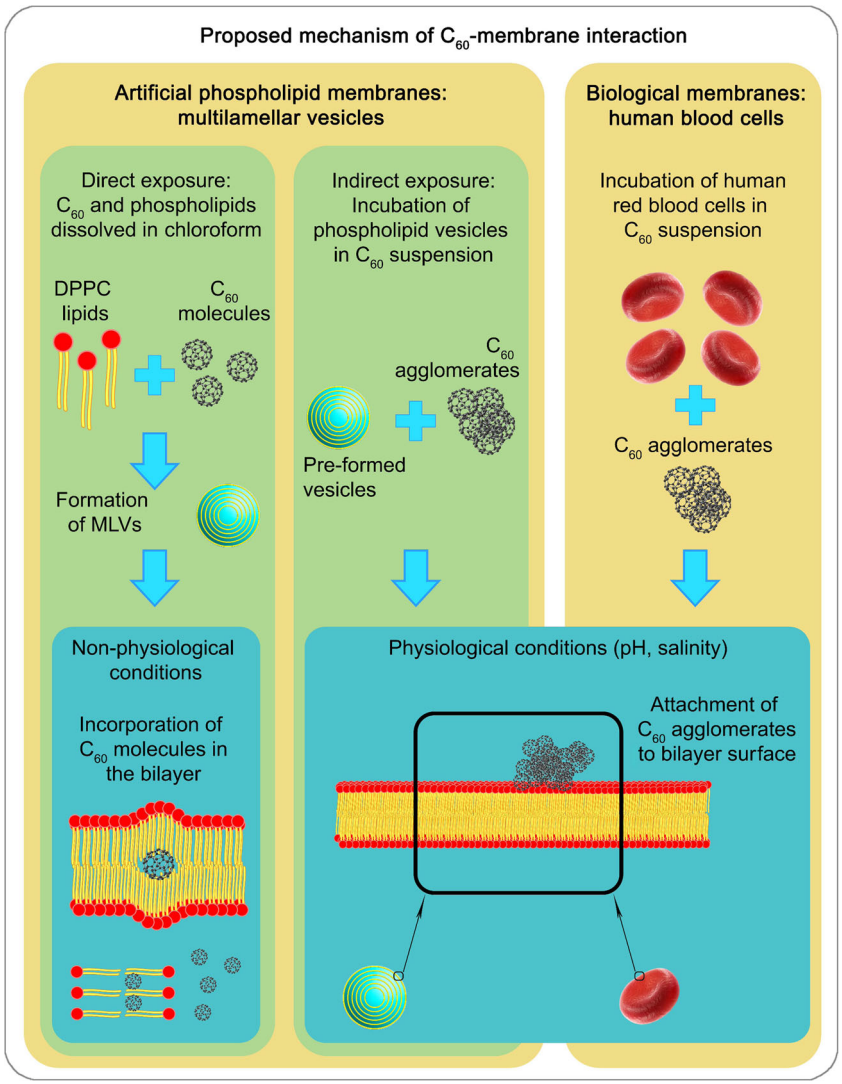

Fig. 4 Schematic presentation of the proposed mechanism of C_{60}-membrane interactions. Two experimental approaches were used: the artificial DPPC phospholipid vesicles were exposed to either C_{60}, dissolved in $CHCl_3$, followed by the formation of MLVs (*left panel*), or pre-formed phospholipid vesicles were incubated in a C_{60} aqueous suspension, where agglomerates of C_{60} were formed (*middle panel*). Similarly, human RBCs were incubated in the C_{60} aqueous suspension (*right panel*). The proposed mechanism of either intercalation of individual C_{60} in the bilayer is presented in the *lower left panel*. The attachment of C_{60} agglomerates, formed in the aqueous suspension, is presented in the *right lower panel*. The software Adobe Photoshop Image 13 was used to create the artwork. The drawing of RBC was used with the Image courtesy of dream designs at FreeDigitalPhotos.net and of C60 with the Image courtesy of James Hedberg at www.jameshedberg.com licensed under http://creativecommons.org/licenses/by-nc-sa/3.0/, with changes: modified color

studies on DPPC and C_{60} reporting that the C_{60} molecules alone or in clusters spontaneously translocate to the hydrophobic core of the membrane and stay inside the bilayer (Bozdaganyan et al. 2014; DeVane et al. 2010; Ikeda et al. 2011; Monticelli et al. 2009; Qiao et al. 2007; Rossi et al. 2013; Shinoda et al. 2012; Wong-Ekkabut et al. 2008). The incorporation of cluster of fullerenes inside the bilayer changes the properties of the bilayer and leads to its deformation (Rossi et al. 2013; Bozdaganyan et al. 2014). Furthermore, with this approach (C_{60} in $CHCl_3$), we have also confirmed that liposomes can be successfully applied as solvents for C_{60} which can serve as a delivering agent for fullerenes to cells, as introduced by the group of Ikeda et al. (Ikeda et al. 2011; Ikeda et al. 2012; Ikeda et al. 2005). When discussing physiological conditions for interactions between fullerenes and lipid membranes, other solvent for fullerenes could be used instead of the non-polar organic solvent ($CHCl_3$). For example, lipid membrane-incorporated fullerenes can be successfully achieved using cyclodextrins (applying exchange reaction method) (Ikeda et al. 2014). Moreover, partitioning of fullerenes inside the membranes has been supported also by MD simulation studies and solubility values of C_{60} (Ruoff et al. 1993). From the thermodynamic point of view, it is favorable for fullerenes to partition into lipid membranes, as discussed by Wong-Ekkabut et al. (2008). They provide estimates on the free energy difference for fullerenes leaving a pure fullerene phase (i.e., large aggregate) and entering the hydrophobic lipid bilayer core. Even if our results show no interaction between aqueous solution of C_{60} and lipid membranes due to large C_{60} clusters formed in the suspension, this does not prove indisputably the absence of interactions between fullerenes and membranes within a different timescale (the DSC measurement was conducted after a 1-h incubation of liposomes in the aqueous suspension of C_{60}.)

We explain that the observed absence of the effect in vitro (physiological conditions), i.e., the incubation of liposomes in the aqueous suspension of C_{60} or the exposure of RBCs to C_{60}

in PBS-citrate buffer, might be due to their formation of large aggregates in polar media (Andrievsky et al. 1995; Fortner et al. 2005; Ruoff et al. 1993; Spohn et al. 2009). The DLS measurements have shown the number distribution of C_{60} clusters in dH_2O to be around 80 nm in diameter, with larger agglomerates (600 to 800 nm) also present. Whereas in both buffers (Hepes and PBS-citrate buffer), representing physiological pH conditions, the major portion of C_{60} agglomerates, larger than 1 μm, could be observed. We explain that when larger agglomerates of C_{60} are formed in a more realistic biological environment (buffers), the number of available clusters or C_{60} agglomerates is reduced, in comparison to suspensions where less agglomeration takes place (e.g., already in dH_2O or in organic solvents, e.g., chloroform). In other words, where larger agglomerates of C_{60} are formed, less active particles are present for the interaction with the biological system, not only with lipids but also with membrane proteins. In our previous study (Mesaric et al. 2013), we applied isolated model membrane proteins, acetylcholinesterase, and tested the enzyme activity in the presence of C_{60} or CB. In line with the observed effect on the shape alterations of RBCs, we observed a very high adsorption of CB on AChE and an inhibition of the enzyme function, whereas the effect of C_{60} on both parameters was almost negligible. We conclude that the effect of carbon NMs may depend on their different surface curvature and, subsequently, on their adsorption potential to interact with biological systems (Mesaric et al. 2013; Xia et al. 2011). The combination of the results of previous and present studies proposes that even though C_{60} did not incorporate in the phospholipid bilayer when liposomes were incubated in the aqueous suspension of C_{60}, under certain conditions, they may compromise the membrane integrity (heating above the T_m 41.6 °C of certain phospholipids). They might also affect membrane proteins and compromise the RBC membrane integrity as a consequence of the interaction with transmembrane band-3 proteins, which are connected to cytoskeletal proteins, responsible for erythrocyte shape (Grebowski et al. 2013), though this was not showed in our study.

Along with the experimental conditions (buffers, media, concentration, exposure time, etc.), also the methodological approach is an important factor to be considered in the assessment of NM-membrane interactions. Zhang et al. (Zhang et al. 2013) reported on the structural damage of the human RBC membrane due to the infiltration of pristine C_{60} in the membranes, assessed by atomic force microscopy (AFM), although the morphology alterations of RBCs were not seen in the microscopy images. The AFM indentation results implied that the presence of C_{60} was able to weaken the cell membrane and makes it more readily to be pierced, which directly evidences that C_{60} NPs have the ability to change the mechanical characteristics of the RBC membrane. Weakening the membranes of RBCs, caused by massive dosages of C_{60}, can compromise the RBC structure and functionality, similarly to the condition of malaria infection (Zhang et al. 2013). To summarize, we agree that the MD simulation studies are good predictors of NM-phospholipid interactions; thus, the results should not be explained alone without bearing in mind their effect in biological (or at least near-physiological) conditions. On the other hand, the absence of the observed effect of NM in the near-physiological pH conditions does not signify with certainty that the tested material is completely inert towards the biological environment. Though it has been predicted that the first interactions of NM occur on cell membranes, the interaction with the lipid bilayer of the cell membrane is not always required for the interaction. For example, a possible attachment of single particles or their agglomerates to membrane proteins can compromise membrane integrity and thus can alter cell functionality. We have experimentally proven that the selected methodological approach needs to be carefully considered when interpreting the assessed effects of NM on biological systems.

Acknowledgments The research was supported by the Ministry of Education, Science, Culture and Sport of Republic of Slovenia in the scope of the grant "Innovative scheme of co-funding doctoral studies promoting co-operation with the economy and solving of contemporary social challenges" in the scope of the Grant No. 160-21. This project has received funding from the Slovenian Research Agency (ARRS) within Grant Agreement No. J1-4109 and Research Program P4-0121. We want to thank Prof. Dr. Darko Makovec from the Jožef Štefan Institute for the characterization of C_{60} suspensions. We want to express our gratitude to Dr. Matej Hočevar from the Institute of Metals and Technology, for his assistance with scanning electron microscopy.

Research involving human participants This study involved human subjects (RBCs) and was approved by the National Medical Ethics Committee of Slovenia, No. 117/02/10.

Conflict of interest The authors declare that they have no conflict of interest.

References

Andrievsky GV, Kosevich MV, Vovk OM, Shelkovsky VS, Vashchenko LA (1995) On the Production of an Aqueous Colloidal Solution of Fullerenes Journal of the Chemical Society-Chemical Communications:1281-1282

Asharani PV, Sethu S, Vadukumpully S, Zhong SP, Lim CT, Hande MP, Valiyaveettil S (2010) Investigations on the structural damage in human erythrocytes exposed to silver, gold, and platinum nanoparticles. Adv Funct Mater 20:1233-–1242. doi:10.1002/adfm.200901846

Bakry R, Vallant RM, Najam-Ul-Haq M, Rainer M, Szabo Z, Huck CW, Bonn GK (2007) Medicinal applications of fullerenes. Int J Nanomed 2:639–649

Banaszak MMH (2009) Nanotoxicology: a personal perspective. Wiley Interdiscip Rev: Nanomedicine and Nanobiotechnology 1:353–359

Boggs JM (1987) Lipid intermolecular hydrogen-bonding—influence on structural organization and membrane-function. Biochim Biophys Acta 906:353–404. doi:10.1016/0304-4157(87)90017-7

Bouropoulos N et al (2012) Probing the perturbation of lecithin bilayers by unmodified C-60 fullerenes using experimental methods and computational simulations. J Phys Chem C 116:3867–3874. doi:10.1021/Jp206221a

Bozdaganyan ME, Orekhov PS, Shaytan AK, Shaitan KV (2014) Comparative Computational Study of Interaction of C-60-Fullerene and Tris-Malonyl-C-60-Fullerene Isomers with Lipid Bilayer: Relation to Their Antioxidant Effect Plos One 9 doi 10.1371/journal.pone.0102487

Crane M, Handy RD, Garrod J, Owen R (2008) Ecotoxicity test methods and environmental hazard assessment for engineered nanoparticles. Ecotoxicology 17:421–437. doi:10.1007/s10646-008-0215-z

Dellinger A, Zhou ZG, Connor J, Madhankumar AB, Pamujula S, Sayes CM, Kepley CL (2013) Application of fullerenes in nanomedicine: an update. Nanomedicine-UK 8:1191–1208. doi:10.2217/Nnm.13.99

DeVane R, Jusufi A, Shinoda W, Chiu CC, Nielsen SO, Moore PB, Klein ML (2010) Parameterization and application of a coarse grained force field for benzene/fullerene interactions with lipids. J Phys Chem B 114:16364–16372. doi:10.1021/Jp1070264

Drasler B et al (2014) Effects of magnetic cobalt ferrite nanoparticles on biological and artificial lipid membranes. Int J Nanomed 9:1559–1581. doi:10.2147/Ijn.S57671

Fortner JD et al (2005) C-60 in water: nanocrystal formation and microbial response. Environ Sci Technol 39:4307–4316

Frascione D et al (2012) Ultrasmall superparamagnetic iron oxide (USPIO)-based liposomes as magnetic resonance imaging probes. Int J Nanomed 7:2349–2359. doi:10.2147/Ijn.S30617

Gmajner D, Grabnar PA, Znidaric MT, Strus J, Sentjurc M, Ulrih NP (2011) Structural characterization of liposomes made of diether archaeal lipids and dipalmitoyl-L-alpha-phosphatidylcholine. Biophys Chem 158:150–156. doi:10.1016/j.bpc.2011.06.014

Grebowski J, Krokosz A, Puchala M (2013) Fullerenol C(6)(0)(OH)(3)(6) could associate to band 3 protein of human erythrocyte membranes. Biochim Biophys Acta 1828:2007–2014. doi:10.1016/j.bbamem.2013.05.009

Hagerstrand H, Danieluk M, Bobrowska-Hagerstrand M, Iglic A, Wrobel A, Isomaa B, Nikinmaa M (2000) Influence of band 3 protein absence and skeletal structures on amphiphile- and Ca2+-induced shape alterations in erythrocytes: a study with lamprey (Lampetra fluviatilis), trout (Oncorhynchus mykiss) and human erythrocytes. BBA-Biomembr 1466:125–138. doi:10.1016/S0005-2736(00)00184-X

Han YC, Wang XY, Dai HL, Li SP (2012) Nanosize and surface charge effects of hydroxyapatite nanoparticles on red blood cell suspensions. Acs Appl Mater Inter 4:4616–4622. doi:10.1021/Am300992x

Huang WD, Qian KX, Tan HQ, Li WZ (1996) The effect of buckyball C-60 irradiation on the fluidity of erythrocyte membranes. Acta Bioch Bioph Sin 28:321–324

Iglic A (1997) A possible mechanism determining the stability of spiculated red blood cells. J Biomech 30:35–40. doi:10.1016/S0021-9290(96)00100-5

Ikeda A, Kiguchi K, Shigematsu T, Nobusawa K, Kikuchi J, Akiyama M (2011) Location of [60]fullerene incorporation in lipid membranes. Chem Commun 47:12095–12097. doi:10.1039/C1cc14650e

Ikeda A et al (2012) Advantages and potential of lipid-membrane-incorporating fullerenes prepared by the fullerene-exchange. Method Chem-Asian J 7:605–613. doi:10.1002/asia.201100792

Ikeda A, Kiguchi K, Hida T, Yasuhara K, Nobusawa K, Akiyama M, Shinoda W (2014) [70]Fullerenes Assist the Formation of Phospholipid Bice Iles at Low Lipid Concentrations Langmuir 30:12315–12320. doi:10.1021/La503732q

Ikeda A et al (2005) Efficient photocleavage of DNA utilising water-soluble lipid membrane-incorporated [60]fullerenes prepared using a [60]fullerene exchange method. Org Biomol Chem 3:2907–2909. doi:10.1039/B507954c

Kato S, Kikuchi R, Aoshima H, Saitoh Y, Miwa N (2010) Defensive effects of fullerene-C60/liposome complex against UVA-induced intracellular reactive oxygen species generation and cell death in human skin keratinocytes HaCaT, associated with intracellular uptake and extracellular excretion of fullerene-C60. J Photoch Photobio B 98:144–151. doi:10.1016/j.jphotobiol.2009.11.015

Kroto HW, Heath JR, Obrien SC, Curl RF, Smalley RE (1985) C-60—Buckminsterfullerene. Nature 318:162–163. doi:10.1038/318162a0

Leonenko ZV, Finot E, Ma H, Dahms TES, Cramb DT (2004) Investigation of temperature-induced phase transitions in DOPC and DPPC phospholipid bilayers using temperature-controlled scanning force microscopy. Biophys J 86:3783–3793. doi:10.1529/biophysj.103.036681

Leroueil PR, Hong SY, Mecke A, Baker JR, Orr BG, Holl MMB (2007) Nanoparticle interaction with biological membranes: does nanotechnology present a janus face? Accounts Chem Res 40:335–342

Li SQ, Zhu RR, Zhu H, Xue M, Sun XY, Yao SD, Wang SL (2008) Nanotoxicity of TiO(2) nanoparticles to erythrocyte in vitro. Food Chem Toxicol 46:3626–3631. doi:10.1016/j.fct.2008.09.012

Lichtenberg D, Menashe M, Donaldson S, Biltonen RL (1984) Thermodynamic characterization of the pretransition of unilamellar dipalmitoyl-phosphatidylcholine vesicles. Lipids 19:395–400. doi:10.1007/Bf02537400

Lyon DY, Adams LK, Falkner JC, Alvarez PJJ (2006) Antibacterial activity of fullerene water suspensions: effects of preparation method and particle size. Environ Sci Technol 40:4360–4366

Mesaric T et al (2013) Effects of surface curvature and surface characteristics of carbon-based nanomaterials on the adsorption and activity of acetylcholinesterase. Carbon 62:222–232. doi:10.1016/j.carbon.2013.05.060

Monticelli L, Salonen E, Ke PC, Vattulainen I (2009) Effects of carbon nanoparticles on lipid membranes: a molecular simulation perspective. Soft Matter 5:4433–4445. doi:10.1039/B912310e

Peetla C, Stine A, Labhasetwar V (2009) Biophysical interactions with model lipid membranes: applications in drug discovery and drug delivery. Mol Pharm 6:1264–1276

Poklar N, Fritz J, Macek P, Vesnaver G, Chalikian TV (1999) Interaction of the pore-forming protein equinatoxin II with model lipid membranes: A calorimetric and spectroscopic study. Biochemistry-Us 38:14999–15008. doi:10.1021/Bi9916022

Prato M (1997) [60] Fullerene chemistry for materials science applications. J Mater Chem 7:1097–1109. doi:10.1039/A700080d

Qiao R, Roberts AP, Mount AS, Klaine SJ, Ke PC (2007) Translocation of C-60 and its derivatives across a lipid bilayer. Nano Lett 7:614–619

Riske KA, Barroso RP, Vequi-Suplicy CC, Germano R, Henriques VB, Lamy MT (2009) Lipid bilayer pre-transition as the beginning of the melting process. BBA-Biomembr 1788:954–963. doi:10.1016/j.bbamem.2009.01.007

Rossi G, Barnoud J, Monticelli L (2013) Partitioning and solubility of C-60 fullerene in lipid membranes Phys Scripta 87 doi 10.1088/0031-8949/87/05/058503

Rudenko SV (2010) Erythrocyte morphological states, phases, transitions and trajectories. BBA-Biomembr 1798:1767–1778. doi:10.1016/j.bbamem.2010.05.010

Ruoff RS, Tse DS, Malhotra R, Lorents DC (1993) Solubility of C-60 in a Variety of Solvents. J Phys Chem-Us 97:3379–3383

Salonen E, Lin S, Reid ML, Allegood M, Wang X, Rao AM, Vattulainen I, Ke PC (2008) Real-time translocation of fullerene reveals cell contraction. Small 4:1986–1992. doi:10.1002/smll.200701279

Schulz M, Olubummo A, Binder WH (2012) Beyond the lipid-bilayer: interaction of polymers and nanoparticles with membranes. Soft Matter 8:4849–4864. doi:10.1039/C2sm06999g

Shinoda W, DeVane R, Klein ML (2012) Computer simulation studies of self-assembling macromolecules. Curr Opin Struc Biol 22:175–186. doi:10.1016/j.sbi.2012.01.011

Spohn P, Hirsch C, Hasler F, Bruinink A, Krug HF, Wick P (2009) C-60 fullerene: a powerful antioxidant or a damaging agent? The importance of an in-depth material characterization prior to toxicity assays. Environ Pollut 157:1134–1139. doi:10.1016/j.envpol.2008.08.013

Verma A, Stellacci F (2010) Effect of surface properties on nanoparticle-cell interactions. Small 6:12–21. doi:10.1002/smll.200901158

Wang B, Zhang LF, Bae SC, Granick S (2008) Nanoparticle-induced surface reconstruction of phospholipid membranes. Proc Natl Acad Sci U S A 105:18171–18175. doi:10.1073/pnas.0807296105

Wong-Ekkabut J, Baoukina S, Triampo W, Tang IM, Tieleman DP, Monticelli L (2008) Computer simulation study of fullerene translocation through lipid membranes. Nat Nanotechnol 3:363–368

Xia XR et al (2011) Mapping the surface adsorption forces of nanomaterials in biological systems. ACS Nano 5:9074–9081. doi:10.1021/Nn203303c

Zhang X, Zhang Y, Zheng Y, Wang B (2013) Mechanical characteristics of human red blood cell membrane change due to C60 nanoparticle infiltration. Phys Chem Chem Phys 15:2473–2481. doi:10.1039/c2cp42850d

Zupanc J et al (2012) Experimental evidence for the interaction of C-60 fullerene with lipid vesicle membranes. Carbon 50:1170–1178. doi:10.1016/j.carbon.2011.10.030